Evidence for a vacancy–phosphorus–oxygen complex in silicon

2009 J. Phys.: Condens. Matter 21 015802

(http://iopscience.iop.org/0953-8984/21/1/015802)

J. Phys.: Condens. Matter **21** (2009) 015802 (6pp) doi:10.1088/0953-8984/21/1/015802

Evidence for a vacancy–phosphorus–oxygen complex in silicon

S Dannefaer, G Suppes and V Avalos

Department of Physics, University of Winnipeg, 515 Portage Avenue, Winnipeg, MB, R3B 2E9, Canada

Received 20 August 2008, in final form 3 November 2008
Published 2 December 2008
Online at stacks.iop.org/JPhysCM/21/015802

Abstract
Low-energy (∼0.5 MeV) electrons arising from ^{60}Co γ-irradiation were used to create phosphorus–vacancy (PV) pairs and oxygen–vacancy pairs in Czochralski-grown Si. Positron annihilation data show that PV pairs anneal in *two* stages: the commonly observed stage around 125 °C, where one third of the pairs disappear with an activation energy of 0.8 ± 0.2 eV, and a new stage where none disappear, but form PV–oxygen complexes with an activation energy of 2.0 ± 0.2 eV.

1. Introduction

The phosphorus–vacancy complex (E center) was identified five decades ago by means of electron paramagnetic resonance (EPR) [1], and its acceptor level in the band-gap at $E_C - 0.4$ eV was determined by Hall effect measurements [2, 3] (E_C is the conduction band edge). The defect is formed during irradiation at room temperature by migrating monovacancies, but in practice there is always competition between trapping at phosphorus and at the ubiquitous oxygen interstitial impurity; in the latter case, oxygen partially occupies the vacancy (A center) and has an acceptor level at $E_C - 0.17$ eV. EPR can only be used to detect the E center when the Fermi level is below $E_C - 0.4$ eV, i.e. when the center is overall neutral, while EPR can be used to detect the A center only in its negatively charged state, i.e. for the Fermi level above $E_C - 0.17$ eV: consequently the two defect types cannot be detected simultaneously in a given sample. Infrared spectroscopy (IR), on the other hand, can be used to detect the A center in both charge states (neutral and negative) [4], but not to detect the E center. Most experiments using EPR, IR and deep level transient spectroscopy have been on samples with P concentrations in the range of $\sim 10^{14}$–$\sim 10^{16}$ cm^{-3}, which is comparable to the oxygen concentration in float-zone refined Si, but is less by at least two orders of magnitude than that in Czochralski-grown Si.

The thermal stability of (neutral) E centers was investigated using EPR by means of reorientation experiments [5], and yielded an activation energy (0.93 ± 0.05 eV) which matched the annealing of E centers in the 100–150 °C range [2]: however, it was not clear how the EPR signal from PV complexes disappeared. Using a different experimental method (the minority carrier lifetime one) the above 0.9 eV was also found, but there was another annealing with a higher energy of 1.3 eV [6]. A similar result was found using the Hall effect [7], so from all of these experiments it seems that annealing of E centers is not solely a matter of dissociation of E centers. Recent theoretical calculations [8, 9] on the thermal stability of the center in various charge states suggest that only the singly negative state (P^+V^-) is stable enough for practical annealing times: this is in contradiction with EPR measurements on the neutral E center [5].

The present work was motivated by the above mentioned inconsistencies, and positron annihilation was chosen as the experimental technique because it can detect A and E centers in the same sample. Furthermore, samples with much higher P concentration than is acceptable for EPR and IR studies were investigated so to reduce, although not remove, the content of A centers. Low-energy electron irradiation via ^{60}Co irradiation was chosen to avoid creating divacancies whose presence would be a source of considerable uncertainty.

2. Experimental details

P doped (5×10^{15}, 1×10^{17}, and 5×10^{18} cm^{-3}) Czochralski-grown Si wafers with an interstitial oxygen concentration of 1×10^{18} cm^{-3} were irradiated at 8 °C with ^{60}Co γ-quanta (1.1 and 1.3 MeV) to a fluence of approximately 1×10^{19} quanta cm^{-2}. Due to the penetration depth of γ-quanta

in Si, the samples were homogeneously damaged by low-energy Compton-scattered electrons. In the case of isochronal annealing the time was 30 min at each temperature, and the shortest practical time in the isothermal annealing experiments was 3 min.

Lifetime spectra with (5–9) $\times$ 10^7 counts were analyzed using the program RESOLUTION [10], and included a source correction consisting of a 250 ps component with an intensity of 2% arising from the 0.8 μm thick aluminum foil onto which the 15 μ Ci ^{22}NaCl source was deposited. This correction was applied to the unirradiated samples (with minuscule effect), but another correction was applied to the irradiated samples as will be explained in the beginning of the next section.

Doppler data were analyzed in terms of two parameters, S and W. S is defined as the ratio between the number of counts in the 511 $\pm$ 0.7 keV window (center part) of the Doppler broadened annihilation peak, and those in the 511 $\pm$ 4.8 keV window which spans the whole width of the peak. W is the ratio between counts in the 'wing' parts of the annihilation peak, as defined by the ratio between the combined counts in the two windows centered at 511 $\pm$ 3.3 keV, each of width 1.6 keV, and those in the 511 $\pm$ 4.8 keV window. W is particularly sensitive to changes in the high-momentum electron distribution caused by impurities. The nominal values of S and W are 0.500 and 0.023, respectively, both calculated after background subtraction.

A general introduction to positron annihilation can be found in [11], from which it is noted that from lifetime data the positron trapping rate can be calculated. This rate is proportional to the vacancy concentration, and its temperature dependence reveals the net charge of the defect. The trapping rate was calculated from the trapping model [12] assuming a single vacancy-type defect according to

$$\kappa = I_2(\lambda_B - \lambda_2)/(1 - I_2). \quad (1)$$

I_2 is the intensity of the τ_2 component arising from vacancies, λ_B the bulk annihilation rate (1/0.218 ns^{-1}), and $\lambda_2 = 1/\tau_2$. This equation applies to the present case, *except* for measurements below ~100 K, where additional traps become active.

The fraction trapped by vacancies, F, is obtained from

$$F = \kappa/(\kappa + \lambda_B), \quad (2)$$

and enters into the decomposition of the experimentally determined S parameter as

$$S = (1 - F)S_B + FS_V. \quad (3)$$

S_B is the S parameter for the bulk and S_V that for a vacancy-type defect, and defining ΔS as $S - S_B$ and ΔS_V as $S_V - S_B$, it follows that the relative defect-specific parameter $\Delta S_V/S_B$ is given by

$$\Delta S_V/S_B = \Delta S/(FS_B). \quad (4)$$

For the W parameter, equations (3) and (4) hold true with S replaced by W.

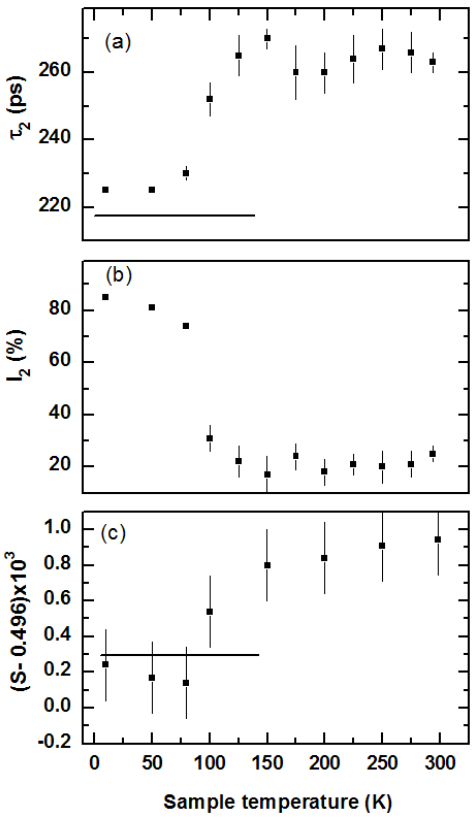

Figure 1. Positron lifetime data (panels (a) and (b)) and the Doppler parameter $(S - 0.496) \times 10^3$ (panel (c)) as a function of sample temperature. The sample was doped with 1×10^{17} P cm^{-3} and irradiated to a fluence of 1×10^{19} γ cm^{-2}. The horizontal line segment in panel (a) at 218 ps indicates the bulk lifetime, and that in panel (c) shows the value for the bulk S parameter.

3. Results

Table 1 lists positron data obtained from samples before and after their irradiation. Unirradiated samples give evidence for a grown-in vacancy-type defect resulting in a lifetime, τ_3, of 370–390 ps with an intensity, I_3, of 5–7%: when analyzing lifetime spectra for the *irradiated* samples the τ_3 lifetime component was removed, technically by treating it as a source correction, so as to determine τ_2 and I_2 properly from the radiation-produced vacancies.

For the least doped samples, the radiation produced a vacancy concentration too small for detection. The intermediately doped samples displayed a rather weak response from vacancies, but nonetheless strong enough to warrant temperature scans and isochronal annealing. In figure 1, panel (a) shows the irradiation-produced lifetime as a function of sample temperature, and panel (b) the intensity of the lifetime component. The S parameter is shown in panel (c). Noteworthy are the correlated changes in the positron parameters, and the same is observed for the highly doped samples (cf figure 3).

Isochronal annealing data are shown in figure 2, where the curve is calculated from data obtained from isothermal annealing of the *highly* doped samples, i.e. a first-order process with an activation energy of 0.8 eV. In the course of the

Table 1. Positron results for unirradiated and irradiated samples. Lifetimes are denoted by τs, and only the corresponding intensities I_2 (I_3) are listed since $I_1 = 100 - I_2$ (I_3). S_B and W_B are the two bulk Doppler parameters, and $\Delta S_V/S_B$ and $\Delta W_V/W_B$ are the relative defect-specific Doppler parameters for the defects created by the irradiation. All measurements were made at room temperature.

Fluence (cm^{-2})	[P] (10^{17} cm^{-3})	τ_1 (ps)	τ_2 (ps)	τ_3 (ps)	I_2 (%)	I_3 (%)	$\Delta S_V/S_B$ (%)	$\Delta W_V/W_B$ (%)
0	0.05	215 ± 2	—	374 ± 30	—	7 ± 2	0	0
	1.0	214 ± 2	—	388 ± 34	—	7 ± 2	0	0
	50	215 ± 2	—	380 ± 20	—	5 ± 1	0	0
1×10^9	0.05	215 ± 2	—	—	—	—	0	0
	1.0	207 ± 3	256 ± 8	—	25 ± 7	—	3 ± 1	—
	50	169 ± 5	261 ± 5	—	59 ± 3	—	3.5 ± 0.2	-10 ± 3

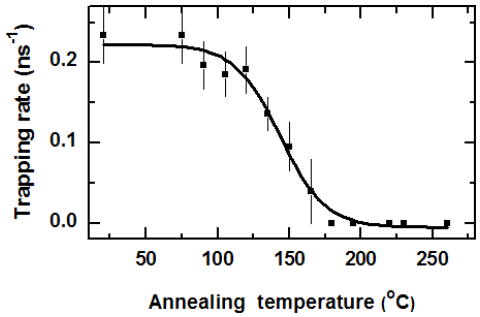

Figure 2. Lifetime data obtained at room temperature for 1×10^{17} P cm^{-3} doped irradiated samples as a function of the 1/2 h isochronal annealing temperature. The curve is generated on the basis of results from *isothermal* annealing of the 5×10^{18} P cm^{-3} doped samples.

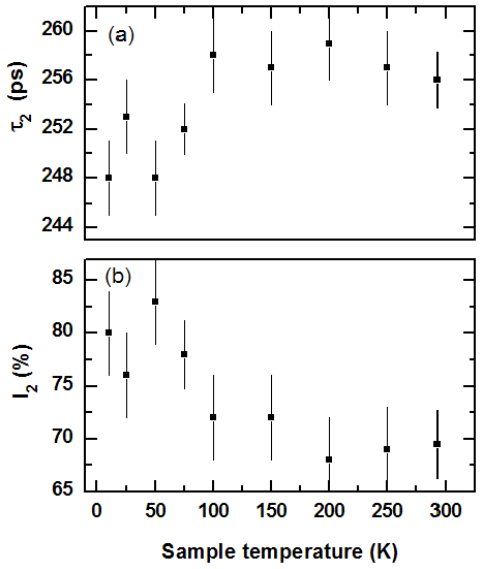

Figure 3. Positron lifetime data as a function of sample temperature for a 5×10^{18} P cm^{-3} doped irradiated sample.

annealing, the values of the radiation-produced τ_2 lifetime were scattered within the range indicated in table 1, i.e. 256 ± 8 ps.

Isothermal annealing of the highly doped samples was done for accumulated times in excess of 150 h for seven different annealing temperatures between 100 and 400 °C. In figure 4 we show data for the lowest annealing temperature where the radiation-produced lifetime and trapping rate are shown in panels (a) and (c), respectively, and the relative defect-specific Doppler parameters in panels (b) and (d). Figure 5 shows data for another sample annealed at 150 °C and figure 6 shows the time dependences within the first 3 h of annealing which are not evident in figure 5. For both annealing temperatures the trapping rate and $\Delta S_V/S_B$ decrease significantly and approach asymptotic values. Lifetime and Doppler parameters for long annealing times at various annealing temperatures are collated in table 2. Annealing at 400 °C for 20 min removes all defects detectable with positrons.

Table 2. Lifetime and Doppler data for irradiated samples annealed at various temperatures for long times (50–250 h) so as to reach 'asymptotic' values. Annealing at 100 °C does not lead to an asymptotic value within 250 h. Annealing at 350 °C for 5 h removes all radiation-produced defects detectable with positrons.

Annealing temperature (°C)	τ_2 (ps)	κ_2 (ns^{-1})	$\Delta S_V/S_B$ (%)	$\Delta W_V/W_B$ (%)
100	257 ± 4	0.90 ± 0.05	2.0 ± 0.1	
150	252 ± 3	0.75 ± 0.05	0.9 ± 0.1	
200	257 ± 4	0.70 ± 0.1	1.0 ± 0.1	-3 ± 2
250	246 ± 3	0.60 ± 0.05	1.0 ± 0.1	
300	240 ± 3	0.65 ± 0.05	0.5 ± 0.2	
350	221 ± 2	—	0	10 ± 4

The temperature dependences of the positron lifetime data in figures 1 and 3 are shown using the experimentally obtained intensities while in figures 2, 4, and 5 trapping rates are used, as calculated from equation (1). The reason for that distinction is that at temperatures lower than ~100 K the calculation of the trapping rate using equation (1) would be erroneous due to the trapping by A centers.

4. Discussion

Radiation damage arising from ^{60}Co irradiation originates from Compton-scattered electrons. About 75% of the scattered electrons capable of creating displacement in head-on collisions impart one to three times the displacement threshold (15 eV [13]). Divacancy formation is hence very unlikely in these experiments, and that is why γ-radiation was chosen rather than the usual MeV-range electron beams. Another reason is that γ-radiation ensures that the volume probed using

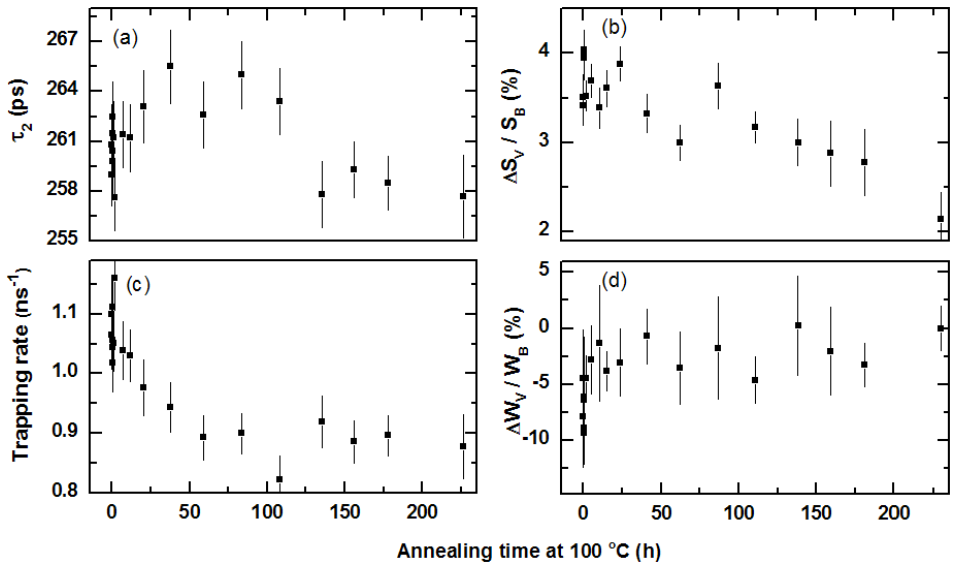

Figure 4. Isothermal annealing at 100 °C of a 5×10^{18} P cm^{-3} doped irradiated sample. Panels on the left contain lifetime data, and those on the right the relative *defect-specific* Doppler parameters. Measurements were done at room temperature.

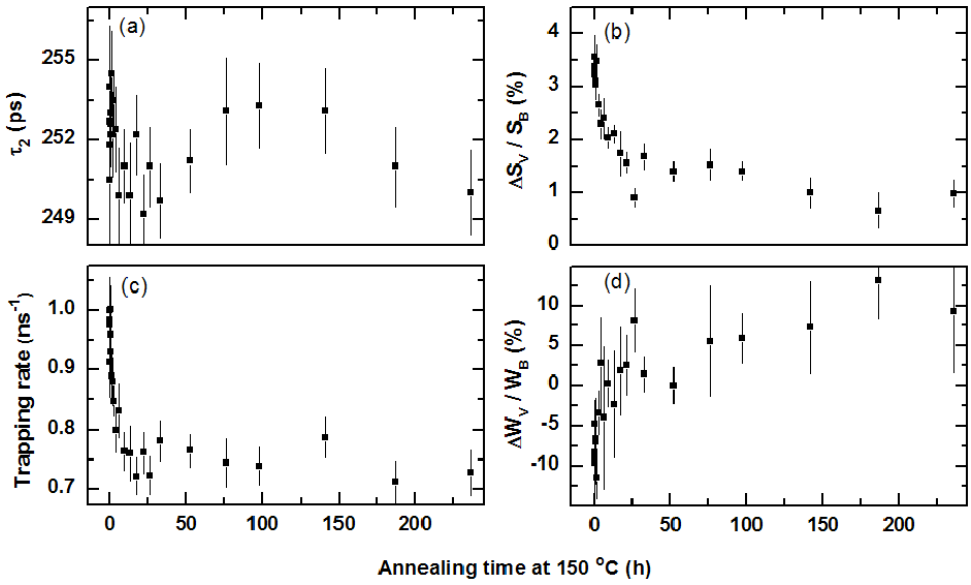

Figure 5. The same as figure 4, but for an isothermal annealing temperature of 150 °C.

the positrons is homogeneously irradiated with low-energy electrons.

Vacancies are doubly negatively charged in our samples, and are trapped either by P^+ or by interstitial oxygen, creating A centers. Positrons detect PV complexes essentially as free vacancies [14] with a lifetime of ∼270 ps, but A centers are weak positron traps, capable of competing with trapping by PV complexes only below ∼100 K, giving a lifetime of ∼220 ps [15]; this trapping is the reason for the positron lifetime and Doppler behaviors below 100 K.

In the least P doped samples the positron data indicate that all of the vacancies created by the radiation are trapped by oxygen. This is expected since the relative trap concentration, [P]/([P] + [O]), is essentially zero. For the intermediately doped samples the above ratio has a value of 0.1, and the trapping rate is ∼0.2 ns^{-1} (at 293 K), while in the highly doped samples the ratio is 0.8, and the trapping rate is ∼1.0 ns^{-1}. The increase in trapping rate reflects the increase in the ratio; the increase by a factor of 8 in the trap concentration ratio results, however, only in an increase in trapping rate by a factor of 5. The reason is most likely that the PV pair in the intermediately P doped samples has a lesser screened Coulomb attractive potential, and hence more effectively traps positrons than in the highly doped samples.

In the highly doped samples the trapping rate corresponds to a concentration of $(1 \pm 0.3) \times 10^{17}$ cm^{-3} [15] assuming that positrons 'see' PV complexes as neutral: this assumption is reasonable because the negative charge is screened by

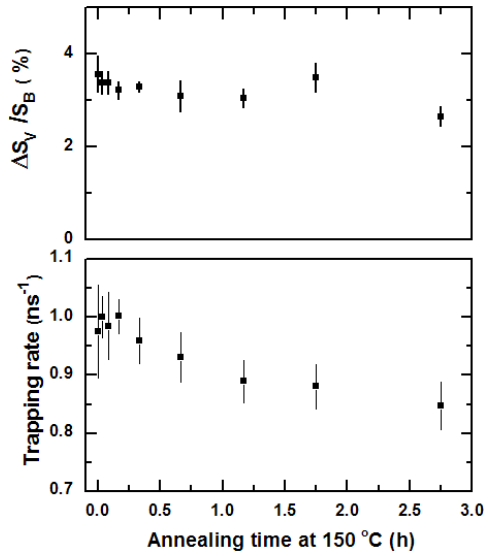

Figure 6. Detail at small annealing times of the data shown in figure 5.

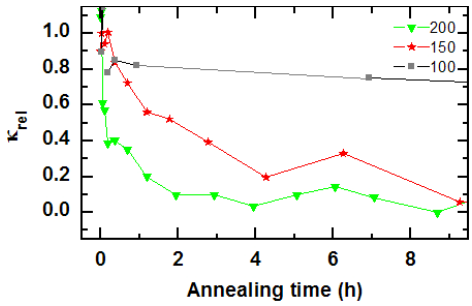

Figure 7. Lifetime data used to yield the activation energy for removing vacancies in the fast stage. Isothermal annealing temperatures are in °C. The parameter $\kappa_{\rm rel}$ is $(\kappa(t)-\kappa_\infty)/(\kappa_0-\kappa_\infty)$ where $\kappa(t)$ is the trapping rate after some annealing time, κ_0 that for zero time, and κ_∞ that after a very long time of annealing.

(This figure is in colour only in the electronic version)

the very high free-carrier density. According to Oen and Holmes [16], the maximum concentration would be 4×10^{17} for a displacement threshold energy of 15 eV [13], indicating a rather large survival rate (∼25%) of the primary created vacancy–interstitial pairs. In view of a similarly high survival rate (∼50%) in 10 MeV electron irradiated highly P doped Si [17], this suggests that stress fields and/or a (screened) Coulomb field could be factors that suppress recombination of vacancy–interstitial pairs shortly after their formation. This implies that vacancies survive in particular within regions of high impurity concentration, as also proposed for the radiation damage in nitrogen doped diamond [18].

Isothermal annealing of the highly doped samples is characterized by two regimes. In the first the trapping rate decreases within a few hours of annealing time while $\Delta S_{\rm V}/S_{\rm B}$ is nearly constant (cf figure 6). In the second regime the trapping rate is nearly constant while $\Delta S_{\rm V}/S_{\rm B}$ and $\Delta W_{\rm V}/W_{\rm B}$ slowly change over long annealing times. The two regimes are, therefore, dominated by two physically different processes.

In the first regime the activation energy for the removal of vacancies is determined from plots of $(\kappa(t)-\kappa_\infty)/(\kappa_0-\kappa_\infty)$ versus annealing time at various temperatures, where κ_0 is the trapping rate for zero annealing time and κ_∞ is the trapping rate for long annealing times. The energy (enthalpy) is calculated from

$$E=\frac{T_1T_2}{1.2\times10^4(T_1-T_2)}\ln(t_2/t_1)\ [\mathrm{eV}], \tag{5}$$

where T_1 and T_2 are two isothermal annealing temperatures and t_1, t_2 the times of annealing at T_1 or T_2, respectively, necessary to produce the same decrease in $(\kappa(t)-\kappa_\infty)/(\kappa_0-\kappa_\infty)$. On the basis of the data shown in figure 7 the activation energy is 0.8 ± 0.2 eV, and the annealing process is of first order; the isochronal annealing data for the 1×10^{17} P cm^{-3} doped sample are satisfactorily fitted using these data (cf figure 2). The experiment does not reveal the nature of the annealing of the PV^- complexes.

Annealing in the second regime is *not* a matter of removal of vacancies, because the trapping rate is nearly constant, but is rather a matter of formation of a new complex because $\Delta S_{\rm V}/S_{\rm B}$ decreases, and this complex is oxygen related, since oxygen is known to reduce the S parameter [15]. Hence, the data suggest that PV^- complexes migrate to oxygen interstitials, forming complexes in which the average electron density is nearly that of the isolated PV^- complex, but with a wider average electron momentum distribution causing $\Delta S_{\rm V}/S_{\rm B}$ to decrease. $\Delta W_{\rm V}/W_{\rm B}$ behaves trivially oppositely to that for $\Delta S_{\rm V}/S_{\rm B}$, *except* that the asymptotic value is +10% (table 2), whereas for $\Delta S_{\rm V}/S_{\rm B}$ it is only (0–1%). That supports the PV^-O model since W emphasizes the momentum contribution from oxygen core electrons.

Doppler isothermal annealing data obtained at 100, 150, 200, and 250 °C are suitable for determining the *formation* energy of the PV^-O complex. Let $\Delta S(PV^-)/S_{\rm B}$ and $\Delta S(PV^-O)/S_{\rm B}$ be the relative defect-specific parameters for the indicated defect complexes, having values of 3.5% and 1.0%, respectively, according to table 2. Then the experimentally obtained $\Delta S_{\rm V}/S_{\rm B}$ parameter is a weighted average of the above two parameters according to the concentration ratio $[PV^-]/[PV^-O]$. Since the trapping rate is constant it is reasonable to assume that *each* PV^- complex that has migrated to O converts into a PV^-O complex with a thermally activated rate, $R=R_0\exp(-E/k_{\rm B}T)$, where E is the sought-for activation energy. R is then determined from experiment via

$$R=(\mathrm{d}/\mathrm{d}t)\ln\{(\Delta S_{\rm V}/S_{\rm B}-\Delta S(PV^-O)/S_{\rm B})/(\Delta S(PV^-)/S_{\rm B}-\Delta S(PV^-O)/S_{\rm B})\}. \tag{6}$$

In the above equation only $\Delta S_{\rm V}/S_{\rm B}$ depends on the annealing time, and for the four usable temperatures, $\ln R$ versus $1/T$ is shown in figure 8. The straight-line fit yields a value of 2.0 ± 0.2 eV.

This activation energy is considerably larger than the reorientation energy (0.93 eV) of the *neutral* PV complex as determined from electron paramagnetic resonance [5] (PV^- is not detectable using this technique). This can mean either that the migration energy of PV^- is 2 eV, or (more likely)

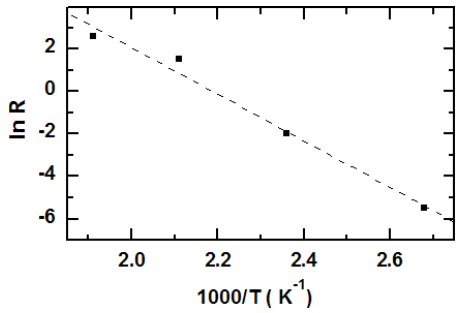

Figure 8. Arrhenius plot of the rate at which PV^-O complexes are formed, based on $\Delta S_V/S_B$ data for four different isochronal annealing temperatures.

that the migration energy is less than 2 eV (1.2 eV according to [7]), but there is a barrier of 2 eV against complex formation suggesting considerable rearrangement of the three individual defects. The complex is stable at 250 °C for at least 250 h, but at 300 °C or above, a steady evolution of new complexes with lesser vacancy character takes place, as indicated by the decrease in positron lifetime (cf table 2 for asymptotic values). Several processes can be envisaged, but a transformation of the PV^-O complex into one where the originally interstitial oxygen occupies the vacancy seems a distinct possibility, i.e. formally a dopant-trapped A center.

5. Conclusion

Annealing of PV^- is characterized by two physically different mechanisms: a well known low-temperature regime close to 125 °C with an activation energy of 0.8 ± 0.2 eV, as for neutral PV complexes, and another one associated with complexing with oxygen, requiring an activation energy of 2.0 ± 0.2 eV. This complex has eluded detection by means of EPR and IR. The complex is stable at 250 °C for at least 250 h, but new complexes evolve with lesser vacancy character at higher temperatures, and no positron traps survive annealing at 400 °C for 20 min.

Acknowledgments

This work was financially supported by the Natural Science and Engineering Research Council of Canada (NSERC). We thank in particular Nordion, MRD, for providing three months of ^{60}Co irradiation via the Canadian Irradiation Facility (Y Doyles).

References

[1] Watkins G D, Corbett J W and Walker R M 1959 *J. Appl. Phys.* **30** 1198
[2] Saito H and Hirata M 1963 *Japan. J. Appl. Phys.* **2** 678
[3] Hirata M, Hirata M, Saito H and Crawford J H Jr 1967 *J. Appl. Phys.* **38** 2433
[4] Lindström J L and Svensson B G 1986 Oxygen, carbon, hydrogen, and nitrogen in crystalline silicon *Mater. Res. Soc. Symp. Proc.* vol 59, ed J C Mikkelsen Jr, S J Pearton, J W Corbett and S J Pennycook (Warrendale, PA) p 45
[5] Watkins G D and Corbett J W 1964 *Phys. Rev.* A **134** 1359
[6] Hirata M, Hirata M and Saito H 1969 *J. Phys. Soc. Japan* **27** 405
[7] Kimerling L C, DeAngelis H M and Diebold J W 1975 *Solid State Commun.* **16** 171
[8] Liu X-Y, Windl W, Beardmore K M and Masquelier M P 2003 *Appl. Phys. Lett.* **82** 1839
[9] Ganchenkova M G, Borodin V A and Nieminen R M 2005 *Nucl. Instrum. Methods Phys. Res.* B **228** 218
[10] Kirkegaard P, Petersen N J and Eldrup M 1989 *PATFIT-88 Risø M-2760* Risø, DK-4000 Roskilde, Denmark
[11] Krause-Rehberg R and Leipner H S 1999 *Positron Annihilation in Semiconductors* (Berlin: Springer)
[12] West R N 1973 *Adv. Phys.* **22** 263
[13] Corbett J W and Bourgoin J C 1975 *Point Defects in Solids* ed J H Crawford and L F Slifkin (New York: Plenum)
[14] Mäkinen J, Hautojärvi P and Corbel C 1992 *J. Phys.: Condens. Matter* **4** 5137
[15] Mascher P, Dannefaer S and Kerr D 1989 *Phys. Rev.* B **40** 11764
[16] Oen O S and Holmes D K 1959 *J. Appl. Phys.* **30** 1289
[17] Avalos V and Dannefaer S 1998 *Phys. Rev.* B **58** 1331
[18] Davies G, Lawson S C, Collins A T, Mainwood A and Sharp S J 1992 *Phys. Rev.* B **46** 13157